Theoretical Calculation of Activation Energies for Pt + H^+(aq) + e^-(*U*) ↔ Pt−H: Activation Energy-Based Symmetry Factors in the Marcus Normal and Inverted Regions

Alfred B. Anderson,* Reyimjan A. Sidik, and Jayakumar Narayanasamy

Chemistry Department, Case Western Reserve University, Cleveland, Ohio 44106

Paul Shiller

Delphi Packard Electric Systems, P.O. Box 431, Warren, Ohio 44486

Received: October 1, 2002; In Final Form: March 13, 2003

The low coverage reversible potential for underpotential deposition of hydrogen on platinum in acid electrolyte is calculated quantum mechanically with two approaches, (i) one using the calculated reaction energy for the overall reaction and an added constant and (ii) the other based on a model of the electrochemical interface. The former yields 0.40 V and the latter 0.48 V, both close to the observed value of ∼0.40 V. Electrode-potential-dependent activation energies are calculated using the interface model for the reduction of the hydronium ion to form the Pt−H bond and for the reverse oxidation reaction over the −0.3 to 3.0 V range. To make this possible, the model explicitly excludes the hydrogen evolution reaction at the cathodic end and water oxidation at the anodic end of the potential range. Cathodic and anodic symmetry factors are determined from the slopes of the activation energy curves, which are used as models for the corresponding activation free energy curves. They are extended into the Marcus-inverted regions for oxidation and reduction. The symmetry factors add to 1.0 in the normal region and in the inverted regions and are not linear functions of the electrode potential.

Introduction

It has long been known from cyclic voltammetric studies that hydrogen undergoes underpotential deposition (upd) on polycrystalline and low-index Pt (111), (100), and (110) surfaces between 0 and about 0.4 V (on the standard hydrogen scale, which is the scale used throughout this paper). Recent infrared−visible sum frequency generation (SFG) spectroscopic analysis of Pt−H vibrations on these electrodes in dilute sulfuric acid indicated that H was terminally bonded to Pt surface atoms in the upd potential range and that these adsorbed H atoms coordinated H_2O molecules to them by hydrogen bonds.[1] In the SFG study the electrodes were also examined in the 0 to −1 V overpotential range, and new spectral features were observed and assigned to vibrations of two H atoms on single-surface Pt atoms. It was noted that the such dihydride structures should be considered as possible intermediates in the hydrogen evolution reaction (HER).

The theme of the present paper is upd hydrogen. Electrode-potential-dependent activation energies (E_a) will be calculated for reducing the hydronium ion, H_3O^+, to generate the Pt−H bond and for the reverse reaction, oxidizing the Pt−H bond to generate the hydronium ion. It will then be shown how the cathodic and anodic symmetry factors as based on these E_a vary with electrode potential in the upd potential ranges. By restriction of the reaction model to exclude other reactions, such as hydrogen evolution and water oxidation, the predictions of E_a-based symmetry factors will be extended into the cathodic and anodic Marcus-inverted regions of electrode potential.[2] The inverted regions are ill-defined over the platinum electrode, platinum being a metal and not a narrow band gap semiconductor, but a discussion of them is possible within the theoretical model being used.

To set the stage for this study a further discussion of the properties of hydrogen on platinum is needed. Hydrogen adsorption on transition metal surfaces has been reviewed recently, and a near equality between Pt−H adsorption bond strengths at the ultrahigh vacuum (UHV) and electrochemical interfaces was noted.[3] As tabulated in ref 3, at the vacuum interface on Pt (111) the Pt−H bond strength, based on measurements of the initial heats of H_2 adsorption, is 237.5 or 259 kJ mol^{-1}; on Pt(100), the Pt−H bond strength is 263.5 kJ mol^{-1}; and for Pt (110), a range of 253−270 kJ mol^{-1} is quoted. A recent analysis of cyclic voltammograms in the hydrogen upd potential range obtained for polycrystalline platinum in weak sulfuric acid has produced Pt−H bond strength values ranging from 265 kJ mol^{-1} at low coverage to 245 kJ mol^{-1} at the high-coverage limit, 0.90 monolayer.[4] It is notable that the surface Pt−H bond strengths vary around 10% with coverage and crystal face and the values for the vacuum and electrochemical interfaces fairly well coincide with one another.

No activation energies (E_a) for Pt−H formation by hydronium ion reduction or for Pt−H oxidation are explicitly known. Apparent E_a for the HER or hydrogen oxidation reaction (HOR) have been determined at 0 V, the reversible potential, from the temperature-dependent exchange current densities for the three low index Pt surfaces in weak sulfuric acid.[5] The values of these E_a are 18 kJ mol^{-1} for Pt (111), 12 kJ mol^{-1} for Pt (100), and 9.5 kJ mol^{-1} for Pt (110). The rate-limiting step was assumed to be H_2 formation by combination of adsorbed H atoms (the

* Corresponding author. Telephone: 216 368 5044. Fax: 216 368 3006. E-mail: aba@po.cwru.edu.

10.1021/jp0271099 CCC: $25.00
Published on Web 04/22/2003

Tafel−Volmer, or T−V, mechanism) or the reduction of hydronium ions over adsorbed H atoms (the Heyrovsky−Volmer, or H−V, mechanism) and not the hydronium ion reduction that generates the adsorbed H. The E_a for H_2 adsorption and desorption have not been found either experimentally or theoretically for the vacuum interface. A small variation in the H adsorption bond strengths at the 1-fold, bridging, and 3-fold hollow sites has recently been calculated theoretically, and this supported the hypothesis that at room-temperature H atoms are mobile on the surface in the vacuum interface.[6]

An attempt to assign the HER mechanism for the three low-index Pt electrode surfaces in 0.05 M H_2SO_4 has been made in ref 5. From the structures of the Tafel slopes (slopes of electrode potential vs log of current density), the T−V mechanism was assigned to Pt (110) and the H−V mechanism was assigned to Pt (100). An unambiguous assignment could not be made for Pt (111). At the least, it is concluded from the studies in ref 5 that at 0 V the E_a for the reaction

$$\mathrm{Pt} + \mathrm{H^+(aq)} + \mathrm{e^-}(U°) \rightarrow \mathrm{Pt{-}H} \qquad (1)$$

is small and no greater than 0.1−0.2 eV on the three low-index platinum surfaces. Within the upd range, E_a for reduction is expected to increase as the electrode potential increases, and for oxidation it is expected to decrease.

Theoretical Approach

It is assumed that an electron will transfer to the electrode (oxidation) or from it (reduction) to the reaction center complex, which in the present case includes a Pt atom of the electrode, when the electron affinity (EA) of the reaction center or its ionization potential (IP) equals the negative of the potential applied to the electrode as measured on the physical (vacuum) scale. The approach is reminiscent of the early radiationless electron tunneling formalism of Gurney[7] and the electron transfer theory of Marcus.[2] On the electrochemical scale this equality takes the form

$$\mathrm{EA\ or\ IP} = (4.6 + U/\mathrm{V})\ \mathrm{eV} \qquad (2)$$

where 4.6 eV is the work function of the standard hydrogen electrode.[8] This approach was first used in conjunction with ab initio calculations to analyze an electrochemical reaction a few years ago.[9] In that early work the formation of H_2 by the H−V mechanism over H-terminated diamond was studied and an explicit electron donor of adjustable IP was added to the Hamiltonian to allow the reduction reaction to be modeled at different potentials. In work since then the donor or acceptor species have not been added to the Hamiltonian; rather, calculations have been performed to determine surfaces of constant EA (for reduction) or IP (for oxidation) corresponding to the electrode potentials of interest, and the lowest energy structures on these surfaces have been assigned as the transition states for the reaction centers at those potentials. Small reaction center models are used because they offer significant advantages over larger ones, as long as bond strengths to the small model electrode sites are close to the experimental values for the extended electrode surface. They are: (i) The electron transfer is to or from the local reaction center without the loss of potential control that might take place for large surface models with near-bulk workfunctions. In such unfavorable cases the electron transfer can take place to or from the cluster irrespective of the structure of the reaction center. (ii) Small cluster models avoid two computational difficulties, long computational time since two calculations are required for each EA or IP point, and difficulties in converging to the ground state that occur with large clusters with many near degeneracies. With these modifications, the model was more recently employed to calculate the potential dependencies of activation energies for the four one-electron steps in O_2 reduction outer-sphere and coordinated 1-fold to Pt.[10,11] Most recently, advancements have been made to take into account the double layer bonding interactions and the contributions of ions in the electrolyte to the reaction center Hamiltonian. These are being introduced in several studies, among them the oxidation of H_2O bonded to Pt,[12] O_2 reduction on the Pt dual site,[13] and CO oxidation on Pt.[14,15]

During the reduction of the hydronium ion over a Pt atom, the $O{-}H^+$ bond is broken and the Pt−H bond is formed. The immediate product, H_3O, cannot retain an $H^•$ because the electron can only go into the O−H σ^* orbital, and this reduces the O−H bond order to $^1/_2$, rendering the OH bond very weak. The $H^•$ is easily released and readily forms a bond to Pt with a bond order of 1 in place of the initial weak hydrogen-bonding interaction. Because of this, it is expected that the transition state will coincide with the electron transfer, as was the case in the past studies.[9−15] The accuracy of the theoretical description of this process depends on (i) the accuracy of the Pt−H bond strength, (ii) the accuracy of the $O{-}H^+$ bond strength, and (iii) the accuracy of the electrostatic potentials from electrolyte ions and surface charges that are included in the Hamiltonian. A check of point i is as follows. On the basis of using a single Pt atom and the MP2 approach with an effective core potential and the Los Alamos double-ζ (LANL2DZ) basis set for Pt and the 6-31G** basis set for light atoms in the Gaussian 94 program,[16] which is the approach used for all calculations in this paper, the calculated Pt−H bond strength for the diatomic molecule D_e is 3.14 eV. The experimental value is uncertain for the diatomic molecule, with $D_e \leq 3.58$ eV.[17] The maximum D_o values for the surfaces are 2.80 eV for the vacuum interface[3] and 2.75 eV for the electrochemical interface.[4] Adding the diatomic zero point vibrational energy of ~0.14 eV[17] to these values yields the respective D_e values of ~2.94 and ~2.89 eV for the electrochemical interface. The present calculations with the diatomic Pt−H model are only 0.2 eV larger. It is noted that the zero point energy for the $O{-}H^+$ diatomic molecule is about 0.19 eV,[18] and since this is within 0.05 eV of the diatomic Pt−H value, the calculated D_e values will be used in the discussion of the reaction energy that is presented below.

The accuracy of the $O{-}H^+$ bond strength, point ii, depends essentially on the treatment of solvation of the hydronium ion because MP2 calculations are intrinsically very accurate for molecules such as this, with errors expected to be 0.2 eV and less.[10] As was shown in ref 10, the solvation stabilization of the hydronium ion is well approximated by hydrogen bonding three isolated (gas phase) H_2O molecules to it. Were the hydronium ion solvated instead by water in the liquid phase, there would be a perturbation of the hydrogen bond network in the water, but this should be a few tenths of an electronvolt at most.[10]

Point iii, determining the effects of ions in the electrolyte on the reaction complex, has recently been shown to be approachable by adding an electrostatic potential to the Hamiltonian for the reaction complex.[12] The potential contribution to the reaction center is approximated by calculating the Madelung sum of potential contributions from all the ions in the electrolyte by assuming they have, on average, a regular rocksalt structure. Formulas are available for different structures and terminations of the ion array,[19] and they yield Madelung sums that are not

strongly dependent on the average structure model used for the electrolyte: Madelung constants are 1.682 for a surface ion center on rocksalt (100), 1.538 for the (110) surface, and 1.648 for an ion center on the cesium chloride (110) surface. The distance between the hydronium ion center and chloride or perchlorate centers is about 9.40 Å in 1.0 M solution. The Madelung sum is then represented by a point charge of −1 e placed 9.40 Å from the center of the hydronium ion in a direction away from it and the metal bonding site. The sum for a 0.1 M monoprotic acid would be a charge of −1 e placed 20.25 Å away or a charge of $-^1/_2$ e placed 10.125 Å away. The structures of double layers are not generally known, but, as discussed in ref 12, a charge of $-\ ^1/_2$ e placed 10 Å away results in the accurate calculation of the reversible potential for the oxidation of H_2O bonded to Pt to OH bonded to Pt and also reasonable values of E_a. The same point charge model is used in this paper.

Results and Discussion

a. Reversible Potentials for Outer Sphere H^+(aq) Reduction. The purpose of this section is to show that reversible potentials for H^+(aq) reduction reactions can be accurately determined from the calculated reaction energy E_r with an added constant representing $P\Delta V$, $T\Delta S$, zero point, and solvation energy contributions for reactions of oxygen-containing molecules in acid solution.[10] This model does not incorporate the $-\ ^1/_2$e point charge discussed in the previous paragraph. Following the procedure in ref 10, the energy of the hydrogen evolution reaction,

$$H^+(aq) + e^-(0) \leftrightarrow {}^1/_2H_2 \quad (3)$$

E_r, is calculated to be − 4.13 eV when H^+(aq) is modeled by variationally optimized $H_3O^+(OH_2)_3$, and the electron energy is zero on the physical scale. On the basis of fitting five other reactions in acid solution in ref 10, the empirical energy to add to this is − 0.49 eV, yielding a ΔG value of − 4.62 eV. Using the relationship between potential and Gibbs energy

$$U = -\Delta G/nF \quad (4)$$

and subtracting 4.60 V to adjust to the electrochemical scale, the predicted reversible potential for eq 3 is 0.02 V, which is very close to the standard value of 0.00 V.

If the reduction is to H• instead

$$H^+(aq) + e^-(0) \leftrightarrow H^\bullet \quad (5)$$

the reversible potential is similarly predicted to be − 2.17 eV, neglecting the presumably small solvation energy of H•. This is close to the thermodynamic estimate of − 2.11 eV in footnote 6 of ref 9.

b. Reversible Potential for upd Hydrogen. The model used in this paper to represent the formation of upd H, a single Pt atom, does not allow a study of the dependence of the reversible potential on H coverage. Using the reaction model

$$Pt{-}OH_2 + H_3O^+(OH_2)_3 + e^-(0) \leftrightarrow Pt{-}H + 5H_2O \quad (6)$$

and adding the −0.49 eV contribution to E_r, the predicted value for $U°$ is 0.40 V. This matches the experimental value of ∼0.40 V at the low-coverage limit.[1,2] As the coverage increases, the average Pt−H bond strength will decrease and the reversible potential for forming additional upd hydrogen will decrease.

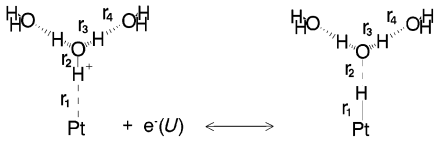

Figure 1. Structure of reaction system drawn to scale and showing the internuclear distances r_1-r_4 that are optimized in the calculations and given in Table 1.

TABLE 1: Structure Parameters for the Reduction and Oxidation Precursors. Internuclear Distances in Å for r_1-r_4 in Figure 1[a]

precursor	r_1	r_2	r_3	r_4
reduction	2.335	0.992	1.024	1.487
oxidation	1.505	1.925	0.963	1.926

[a] The angle θ(HOH) is fixed at the optimized $H^+OH_2(OH_2)_2$ value of 116.6° for both precursors and the orientations, and O−H distances in the two solvating water molecules are also fixed.

A second model for finding the reversible potential for upd H is based on the energy difference for the reaction

$$Pt\cdots H^+OH_2(OH_2)_2 + e^-(0) \leftrightarrow Pt{-}H\cdots OH_2(OH_2)_2 \quad (7)$$

This is an elementary electrochemical interface model with proton or hydrogen atom transport between the surface and the double layer. A $-^1/_2$e point charge is placed 10 Å from the hydronium ion as discussed above. On the left-hand side of eq 7, the hydronium ion, solvated by hydrogen bonding to two H_2O, is hydrogen bonded to Pt. The hydrogen bond strength between Pt and the hydronium ion is 0.42 eV. On the right-hand side of eq 7 there is a hydrogen bond of strength 0.17 eV between H of Pt−H and O of the solvated H_2O. Figure 1 shows eq 7 in greater structural detail, and Table 1 lists the optimized values of the geometric parameters. The reaction energy calculated with this model is 5.45 eV when the energy of the electron is zero on the physical scale. This corresponds to a reversible potential of 0.85 V for this interfacial process. This reduces to 4.88 eV and a reversible potential of 0.18 V when the energy for removing the H_2O molecule to free up a site for the reaction is taken into account. The calculated change in Gibbs energy for eq 7 is 5.67 eV, and taking into account the displacement of H_2O(ads) and vibrational entropy of the Pt−O bond, the overall reaction Gibbs free energy is 5.08 eV, corresponding to a reversible potential of 0.48 V.

The predictions of the reversible potential for forming upd hydrogen including displacing a water molecule, 0.18 V based on the reaction internal energy and 0.48 V based on the free energy are close to the prediction of 0.40 V for eq 6. In the following, symmetry factors will be calculated using internal energies.

c. Dependence of Activation Energies on Electrode Potential. To calculate activation energies that correspond to the 0.18 V reversible potential would require extending the model of eq 7 to include the water molecule that is displaced during the reduction. This would be an enormous computational complication, and to have a complete model for calculating symmetry factors to relate to the Marcus picture, it was not done.

The reduction precursor, $Pt\cdots H^+OH_2(OH_2)$, has an electron affinity of 4.644 eV, corresponding to 0.044 V on the electrochemical scale. Because of the bond order changes that take place upon the transfer of the electron to the reaction center, E_a is, as discussed in the Introduction, zero. As shown in Figure 2, E_a increases as the electrode potential is increased. Taking

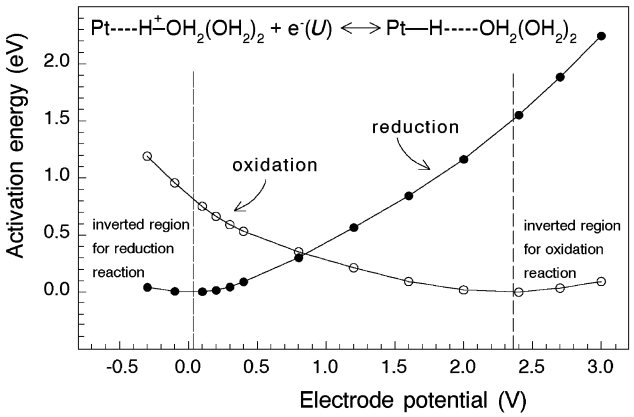

Figure 2. Calculated activation energies for the electrochemical oxidation and reduction reactions involving upd H graphed as functions of electrode potential.

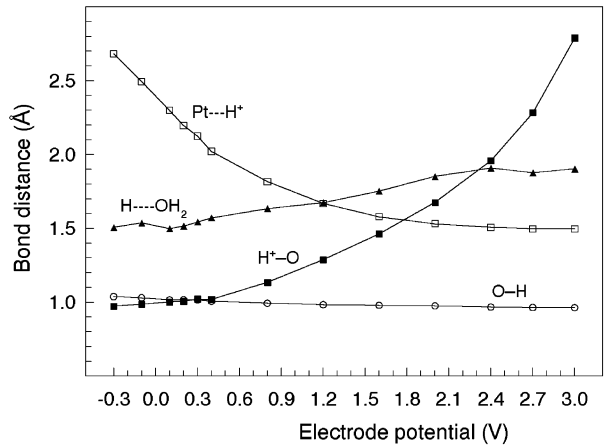

Figure 3. Calculated structure parameter values at transition states at various electrode potentials for the electroreduction reaction.

the E_a as approximations to the Gibbs free energy of activation, G_a, these electrode potentials are in the Marcus "normal" region for the reduction reaction. This increase is the result of changing the structure of the reaction center (parameters are displayed graphically in Figure 3) to produce increasingly larger EA's that are related to U by eq 2. The lowest energy structure with the proper EA is chosen for the transition state. As shown in Figure 3, to increase EA requires stretching the H^+-O bond and shortening the $Pt\cdots H^+$ distance in order to stabilize the empty O−H σ^* acceptor orbital. The two H_2O molecules that are hydrogen bonded to the hydronium ion move away a relatively small amount, lengthening the distance between their lone-pair orbitals and the reduction center. The other two O−H distances in the hydronium ion change very little. At potentials negative of 0.044 V reduction can also take place, and in this region, the EA's become increasingly smaller. Assuming again that $G_a(U) \approx E_a(U)$, these potentials are in the Marcus-"inverted" region for the oxidation reaction and E_a increases as the electrode potential goes further negative into this region. Our model allows the inverted region to be defined because the electron source is allowed to have just one IP corresponding to the electrode potential, which is the Fermi energy, E_f. A metallic electrode would have electrons available below E_f that would reduce the reduction precursor at potentials in the inverted region without activation.

The oxidation precursor, $Pt-H\cdots OH_2(OH_2)$, has an ionization potential of 6.970 eV, corresponding to 2.370 V on the electrochemical scale. Because of bond order changes when the electron leaves the reaction center, E_a is zero at this potential.

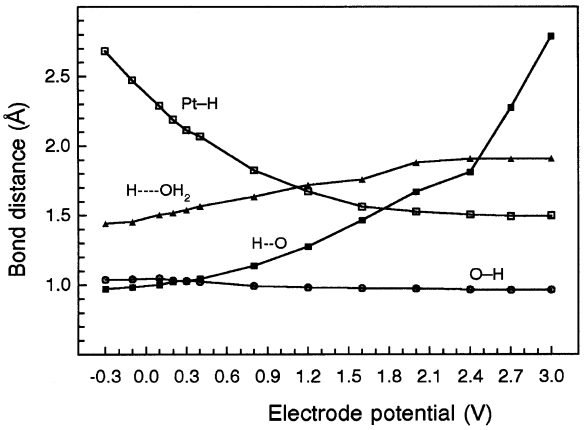

Figure 4. Calculated structure parameter values at transition states at various electrode potentials for the electrooxidation reaction.

The electrode potential range negative of this is the Marcus-normal region for this oxidation reaction and the potential range positive of it is in the Marcus-inverted region for this reaction. The inverted region for oxidation is defined because our model omits excited states above E_f that would oxidize the oxidation precursor at potentials in the inverted region without activation. The curve rises at potentials increasingly negative of the precursor potential and crosses the reduction E_a curve at 0.85 V, the reversible potential for this process. Figure 4 shows the dependence of the structure parameters at the transition states on the electrode potential. The transition state structures are nearly the same, the slight variations being due to carrying out two independent approaches to the transition state at each given electrode potential, one for the reduction reaction and the other for the oxidation reaction.

Symmetry Factors

Symmetry factors are fundamental parameters in electrode kinetics that are defined at constant temperature and pressure. The cathodic symmetry factor, β_c, is the rate of change of the free energy of activation of a reduction reaction G_a^c with overpotential, η_c:

$$\beta_c = (\partial G_a^c/\eta_c)_{T,P} \tag{8}$$

where $\eta_c = U - U^\circ$, so that η_c is <0 V in the electrode potential region that is ordinarily referred to as the overpotential region for a reduction reaction. When η_c is > 0 V, the potential region is referred to as the underpotential region for a reduction reaction. In referring to a specific process, such as O_2 reduction to H_2O at a fuel cell cathode, the underpotential region is not considered, although this would be the overpotential region for H_2O oxidation to O_2. The anodic symmetry factor is

$$\beta_a = -(\partial G_a^a/\eta_a)_{T,P} \tag{9}$$

where $\eta_a = U - U^\circ$ so that η_a is > 0 V in the electrode potential region that is referred to as the overpotential region for an oxidation reaction, and when η_a is <0 V, it is in the underpotential region for such a reaction.

On either side of the equilibrium potential for a given reaction, the η_c and η_a overpotential notations are used in the literature even in the underpotential regions. In traditional Marcus theory, β_c and β_a are $^1/_2$ when η_c and η_a are zero, i.e., at the reversible potential, and they vary linearly with electrode potential. The symmetry factors are related to slopes of Tafel plots (U vs log i, where i is the current density) and $\beta_c(\eta_c)$ and $\beta_a(\eta_a)$ are

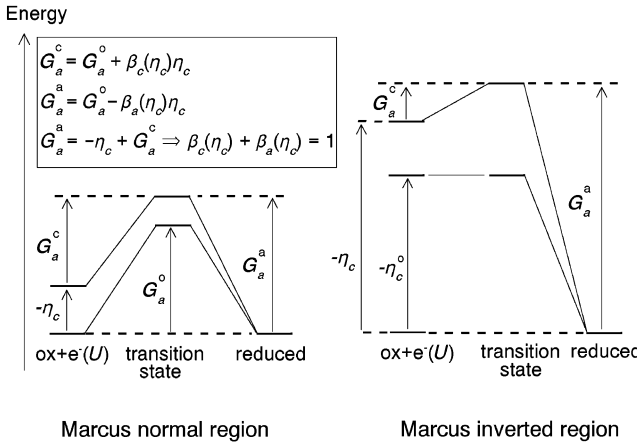

Figure 5. Energy state diagram depicting reactant energy and activation energy for a reduction reaction as functions of cathodic overpotential in the Marcus-normal and -inverted potential ranges. Definitions of symbols are in the text.

generally observed not to change linearly with potential. That the symmetry factors add to 1 in the Marcus-normal region

$$\beta_c(\eta_c) + \beta_a(\eta_c) = 1 \tag{10}$$

is well-known.[20]

Figure 5 provides the explanation for eq 10 for a reduction reaction in the normal region (left side of figure). As $|\eta_c|$ increases (η_c is negative), the energy of the oxidized system plus the electron in the electrode increases and G_a^c, the activation energy for the cathodic reaction, decreases from its value G_a° at the reversible potential by the amount $\beta_c(\eta_c)\eta_c$. The activation energy for the reverse (oxidation) reaction, G_a^a, increases by the amount $-\beta_a(\eta_c)\eta_c$, and, as the figure shows, eq 10 results. Considering the oxidation reaction and increasing the electrode potential from the reversible value, the overpotential range for oxidation, η_a is entered. On doing so, G_a^a will decrease and G_a^c will increase, and again eq 10 is obtained.

As $|\eta_c|$ increases, the cathodic activation energy will decrease to zero at the potential corresponding to the precursor EA. Let this overpotential be denoted η_c°. The right side of Figure 5 shows what happens when the cathodic overpotential is extended beyond η_c°: G_a^c begins to increase. In this potential range G_a^a is also increasing, and by using the fact that $\beta_c = 0$ and $\beta_a = 1$ when $\eta_c = \eta_c^\circ$, eq 10 is again obtained because, in the inverted region for reduction, the cathodic symmetry factor becomes negative. In the inverted region for oxidation the anodic symmetry factor becomes negative, so again eq 10 holds.

Looking at Figure 2, it is seen that in the normal region eq 10 corresponds to taking the slope of the E_a^c curve, a positive number less than 1 and adding to it the negative of the slope of the E_a^a curve. The negative sign is a result of the direction of increasing overpotential for oxidation being reversed on the electrode potential scale.

Symmetry factors determined from slopes in Figure 2 are given in Figure 6. The trends with electrode potential that are established in the normal region continue into the inverted regions. Anodic and cathodic symmetry factors add to 1 in the normal region and in the inverted regions in accordance with eq 10, and they are not linear functions of potential.

Conclusions

Reversible potentials for the reduction of $H^+(aq)$ to $H^\bullet$, H_2, and underpotential deposited H on Pt can be determined accurately using a combination of reaction energies calculated for model systems and a constant that was determined previously for other reactions involving hydrogen and oxygen in acid. The electrochemical interface model, which includes an approximation to the electrostatic contribution to the Hamiltonian at the reaction center that are caused by the counterion to the hydronium ion and other ions in solution, yields a reversible potential for upd H that is in close agreement with the first model. The calculated activation energy is 0.33 eV at the reversible potential for the onset of upd hydrogen formation. Including the energy for displacing a water molecule bonded to the surface, with adsorption energy quoted at 0.65 eV[21] and 0.42 eV[22] in the experimental vacuum literature, shifts the calculated 0.85 V onset potential 0.65 or 0.42 V in the negative direction, closer to the observed onset potential. At higher coverage of hydrogen at lower potentials, the weaker Pt−H bond strength will cause the crossing point and reversible potential to shift further in the cathodic direction according to eq 6. This means that the activation energies at 0 V will be nearly the same for the oxidation or the reduction steps. These results are in qualitative agreement with experiment, and to achieve quantitative agreement will require a much more elaborate model.

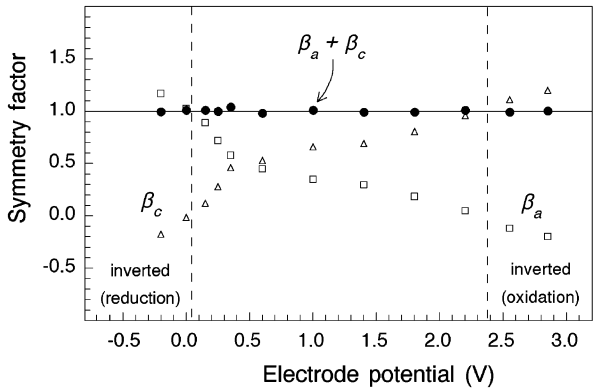

Figure 6. Calculated electrode-potential-dependent cathodic and anodic symmetry factors (β_c and β_a respectively) for upd H and their sum in the Marcus-normal potential region and differences in the Marcus-inverted region.

The cathodic and anodic symmetry factors are found to add to 1 in the normal kinetic region and in the inverted regions, as they must for any reaction according to the analysis in Figure 5. In this general approach, the symmetry factors are not linear in electrode potential as they are in the harmonic model of the Marcus approach.

Acknowledgment. This research is supported by the National Science Foundation, Grant No. CHE-9982179, and by the Army Research Office, Grant No. DAAD19-99-1-0253.

References and Notes

(1) Peremans, A.; Tadjeddine, A. *J. Chem. Phys.* **1995**, *103*, 7197−7203.

(2) Marcus, R. A.; Sutin, N. *Biochim. Biophys. Acta* **1985**, *811*, 265−323.

(3) Christman, K. In *Electrocatalysis*; Lipkowski, J., Ross, P. N., Eds.; Wiley: New York, 1998; pp 1−42.

(4) Zolfaghari, A.; Chayer, M.; Jerkiewicz, G. *J. Electrochem. Soc.* **1997**, *144*, 3034−3041.

(5) Markovic, N. M.; Ross, P. N., Jr. In *Interfacial Electrochemistry*; Wieckowski, A., Ed; Marcel Dekker: New York, 1999; pp 821−842.

(6) Papoian, G.; Norskov, J. K.; Hoffmann, R. *J. Am. Chem. Soc.* **2000**, *122*, 4129−4144.

(7) Gurney, R. W. *Proc, R. Soc.* **1931**, *A 134*, 137−154.

(8) Bockris, J. O'M; Khan, S. U. M. *Surface Electrochemistry*; Plenum Press: New York, 1993; p 493.
(9) Anderson, A. B.; Kang, D. B. *J. Phys. Chem.* **1998**, *102*, 5993−5996.
(10) Anderson, A. B.; Albu, T. V. *J. Am. Chem. Soc.* **1999**, *121*, 11855−11863.
(11) Anderson, A. B.; Albu, T. V. *J. Electrochem. Soc.* **2000**, *147*, 4229−4238.
(12) Anderson, A. B.; Neshev, N. M.; Sidik, R. A.; Shiller, P. *Electrochim. Acta* **2002**, *47*, 2999−3008.
(13) Sidik, R. A.; Anderson, A. B. *J. Electroanal. Chem.* **2002**, *528*, 69−76.
(14) Anderson, A. B.; Neshev, N. M. *J. Electrochem. Soc.* **2002**, *149*, E383−E388.
(15) Narayanasamy, J.; Anderson, A. B. *J. Electroanal. Chem.*, in press.
(16) Gaussian 94 (Revision C. 3). Frisch, M. J.; Trucks, G. W.; Schlegel, H. B.; Gill, P. M. W.; Johnson, B. G.; Robb, M. A.; Cheeseman, J. R.; Keith, T. A.; Petersson, G. A.; Montegomery, J. A.; Raghavachari, K.; Al-Laham, M. A.; Zakrzewski, V. G.; Ortiz, J. V.; Foresman, J. B.; Cioslowski, J.; Stefanov, B. B.; Nanayakkara, A.; Challacombe, M.; Peng, C. Y.; Ayala, P. Y.; Chen, W.; Wong, M. W.; Andres, J. L.; Replogle, E. S.; Gomperts, R.; Martin, R. L.; Fox. D. J.; Binkley, J. S.; Defrees, D. J.; Baker, J.; Stewart, J. P.; Head-Gordon, M.; Gonzalez, C.; Pople, J. A. Gaussian, Inc.: Pittsburgh, PA, 1995.
(17) Huber, K. P.; Herzberg, G. *Molecular Spectra and Molecular Structure IV. Constants of Diatomic Molecules*; van Nostrand Reinhold: New York, 1979 p 546.
(18) Reference 17, p 516.
(19) Magill, J.; Bloem, J.; Ohse, R. W. *J. Chem. Phys.* **1982**, *76*, 6227−6242.
(20) Gileadi. E. *Electrode Kinetics for Chemical Engineers and Materials Scientists*; VCH Publishers: New York, 1993; p 129.
(21) Fisher, G. B.; Gland, J. L. *Surf. Sci.* **1980**, *94*, 446.
(22) Sexton, B. A.; Hughes, A. E. *Surf. Sci.* **1984**, *140*, 227.